Characterization of β-Connectin (Titin 2) from Striated Muscle by Dynamic Light Scattering

H. Higuchi,*‡ Y. Nakauchi,§ K. Maruyama,§ and S. Fujime*

*Graduate School of Integrated Science, Yokohama City University, 22-2 Seto, Kanazawa, Yokohama 236, Japan; ‡Department of Biology, Faculty of Science, Chiba University, 1-33 Yayoi-cho, Inage, Chiba 263, Japan

ABSTRACT Connectin (titin) is a large filamentous protein (single peptide) with a molecular mass of ~3 MDa, contour length ~900 nm, and diameter ~4 nm, and resides in striated muscle. Connectin links the thick filaments to the Z-lines in a sarcomere and produces a passive elastic force when muscle fiber is stretched. The aim of this study is to elucidate some aspects of physical properties of isolated β-connectin (titin 2), a proteolytic fragment of connectin, by means of dynamic light-scattering (DLS) spectroscopy. The analysis of DLS spectra for β-connectin gave the translational diffusion coefficient of 3.60×10^{-8} cm²/s at 10°C (or the hydrodynamic radius of 44.1 nm), molecular mass little smaller than 3.0 MDa (for a literature value of sedimentation coefficient), the root-mean-square end-to-end distance of 163 nm (or the radius of gyration of 66.6 nm), and the Kuhn segment number of 30 and segment length of 30 nm (or the persistence length of 15 nm). These results permitted to estimate the flexural rigidity of 6.0×10^{-20} dyn × cm² for filament bending, and the elastic constant of 7 dyn/cm for extension of one persistence length. Based on a simple model, implications of the present results in muscle physiology are discussed.

INTRODUCTION

From the beginning of its finding (Maruyama et al., 1977), connectin has been considered to be a long and flexible (elastic) filament. Connectin (also called titin) is a large filamentous protein (single peptide) with molecular mass of ~3 MDa, length of ~900 nm, and diameter of ~4 nm, and resides in striated muscle (for reviews see Wang (1985), Maruyama (1986), and Trinick (1991)). Recently, a fraction of the molecular structure of connectin was revealed; connectin has repeats of 100 amino acids in the primary structure (Labeit et al., 1990 and 1992) and of 4-nm domains in the tertiary structure (Funatsu et al., 1993). The 4-nm repeats form 44-nm superrepeats consisting of I-I-I-II-I-I-I-II-I-I-II, with I and II being type III fibronectin and immunoglobulin C_2 motifs, respectively (Labeit et al., 1992). Connectin links the thick filaments to the Z-line in a sarcomere and produces a passive elastic force when muscle fiber is stretched (Funatsu et al., 1990 and 1993; Wang et al., 1991). By producing this passive force, connectin would maintain the regular structure of sarcomeres centering the A-band at the center of a sarcomere and support the tension development (Higuchi and Umazume, 1985; Horowits and Podolsky, 1987; Horowits et al., 1989).

Among muscle filaments, F-actin is semiflexible (Maeda and Fujime, 1980) and a myosin filament is rigid (Mochizuki-Oda and Fujime, 1988). On the other hand, the isolated connectin filament is very flexible (Maruyama et al., 1984) and easily oriented by an external force (Nave et al., 1989). However, few studies have been reported on physical properties of isolated connectin. The aim of this study is to elucidate some aspects of physical properties of connectin by means of dynamic light-scattering (DLS) spectroscopy.

The usual "bead-and-spring" model of Rouse and Zimm for a Gaussian coil (or flexible chain) consists of N Gaussian segments, each of average length b, connecting $N + 1$ identical beads (Yamakawa, 1971). The segments are assumed to provide Hookean restoring forces to the beads. The contour length of the coil is given by $L = Nb$, and its mean-square end-to-end distance is given by $\langle R^2 \rangle = Nb^2 = Lb$. Another model, the so-called "worm-like chain" model of Kratky and Porod (Yamakawa, 1971), considers a continuous space curve with the contour length L and the Kuhn statistical segment length γ^{-1}. For the worm-like chain, $\langle R^2 \rangle$ is given by

$$\langle R^2 \rangle = 2L^2[\exp(-2\gamma L) - 1 + 2\gamma L]/(2\gamma L)^2. \quad (1)$$

Equation 1 becomes $\langle R^2 \rangle = L/\gamma$ for $\gamma L \gg 1$, so that γ^{-1} and γL in the worm-like chain model for large γL correspond, respectively, to b and N in the bead-and-spring model. (On the other hand, Eq. 1 becomes $\langle R^2 \rangle = L^2$ in the limit of $\gamma L \ll 1$, so that a weakly bending (or semiflexible) rod is also modeled by a worm-like chain for $\gamma L < 1$). The DLS spectra for filaments provide us information about dynamics of the segmental motions (or of the internal modes of motion) as well as dynamics of the center-of-mass motion (or the translational diffusion of the filament as a whole) (Pecora, 1968).

In this paper, connectin molecules in solution will be characterized by means of DLS spectroscopy, and qualitative analyses of DLS spectra and implications of the result are discussed. To avoid confusion, the following should be noted. When the words "Gaussian coil" are used for connectin, they mean that the overall shape (or quaternary structure) of a single connectin filament assumes a Gaussian coil; they never mean a random coil conformation in the secondary structure of connectin.

Received for publication 17 May 1993 and in final form 26 July 1993.

Address reprint requests to S. Fujime, Graduate School of Integrated Science, Yokohama City University, 22-2 Seto, Kanazawa, Yokohama 236.

‡Present address: Yanagida Biomotron Project, Exploratory Research for Advanced Technology, Research Development Corporation of Japan, 2-4-14 Semba-higashi, Mino, Osaka 562, Japan.

0006-3495/93/11/1906/10 $2.00

MATERIALS AND METHODS

Preparation of β-connectin

Connectin was prepared in a partially proteolyzed form, called β-connectin (titin 2), from chicken breast muscle as described elsewhere (Itoh et al., 1986). Finally, β-connectin was eluted through a hydroxylapatite column with a solution containing 0.3 M NaCl and 0.25 M potassium phosphate buffer at pH 7.0. Concentration of β-connectin was determined from the absorption at 280 nm calibrated by the absorption coefficient of 1.2 per 1 mg/ml of protein per 1-cm optical path (Maruyama, 1986). β-Connectin was stored on ice and used within 5 days after preparation. For sodium dodecyl sulfate polyacrylamide gel electrophoresis (SDS-PAGE), purified β-connectin and a piece of chicken breast muscle were, respectively, dissolved in lysis solutions (5.5% SDS, 50 mM tris(hydroxymethyl)-aminomethane-HCl, pH 8.0, 10% glycerol and 20 mM dithiothreitol) and then boiled for 1 min. The samples were then loaded on a 1–12% gradient polyacrylamide gel and electrophoresed (Fairbanks et al., 1971). Proteins were stained with Coomassie Brilliant Blue. Contents of proteins were measured from absorbance at 560 nm with a chromatoscanner (CS-9000; Shimadzu Co., Kyoto). Our preparation contained more than 90% β-connectin. Fig. 1 shows SDS-PAGE patterns of whole muscle (*lane 1*) and purified β-connectin (*lane 2*). Unless otherwise stated, connectin means β-connectin in 0.3 M NaCl and 0.25 M potassium phosphate buffer at pH 7.0 throughout this paper.

DLS measurements

General background information about the DLS method is found in standard textbooks (Chu, 1974; Berne and Pecora, 1975; Schmitz, 1990). An (8 by *N*)-bit digital correlator (K7032CE; Malvern Instruments, Malvern, UK) was used to measure the intensity autocorrelation function of the scattered light. A 488-nm beam from an Ar^+ ion laser (Model 95; Lexel Corp., Palo Alto, CA) was used as a light source. Our spectrometer was essentially the same as that detailed elsewhere (Fujime et al., 1984). Unless otherwise stated, the temperature of the scattering sample was kept at 10.0 ± 0.1°C.

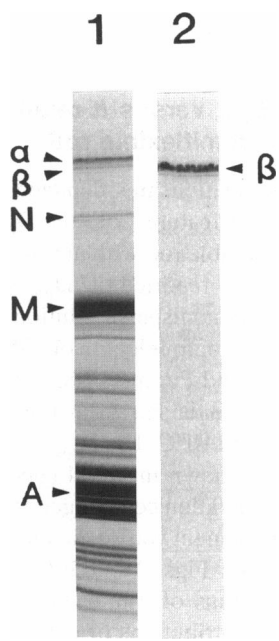

FIGURE 1 SDS-PAGE patterns of the purified β-connectin. Samples were loaded on a 1–12% gradient polyacrylamide gel. Lane 1, total extracts from chicken breast muscle; lane 2, purified β-connectin. α, β, *N*, *M*, and *A* denote α-connectin, β-connectin, nebulin, myosin heavy chain, and actin, respectively.

The intensity autocorrelation function $G^2(t)$ is related to the normalized field correlation function $g^1(t)$ of the scattered light by

$$G^2(t) = B\{\beta[g^1(t)]^2 + 1\}, \quad (2)$$

where $t = mt_s$ ($m = 1, 2, \ldots, 256$; t_s, the sampling time), B is the baseline level, and β is a constant (about 0.7 in our optical setup). For a monodisperse suspension of small particles, we have a simple form of $g^1(t) = \exp(-DK^2t)$, where D is the translational diffusion coefficient of the particle and K is the length of the scattering vector, which equals $(4\pi/\lambda)\sin(\theta/2)$ (λ, the wavelength of light in the medium; θ, the scattering angle). The actual form of $g^1(t)$ of our system is a sum of exponential decays because of possible contributions to the decay of $g^1(t)$ from conformation fluctuations (internal modes of motion) and length distribution of scatterers. Then, the following expansion method is used to obtain a measure of the average decay rate $\langle\Gamma\rangle$;

$$g^1(t) = (1 + m_2t^2 - m_3t^3)\exp(-\langle\Gamma\rangle t). \quad (3)$$

The quantity $\langle\Gamma\rangle/K^2$ has the same dimension as that of D (cm^2/s) and is called an apparent diffusion coefficient, D_{app}.

Theoretically speaking, the apparent diffusion coefficient is given by

$$D_{app} = D + \Sigma' D_{[n]}a_n(x) \quad (4)$$

for Gaussian coils (Fujime and Higuchi, 1993), and

$$D_{app} = D + (R \text{ and } A \text{ terms}) + \Sigma'' D_{[m]}b_m(k) \quad (5)$$

for semiflexible rods (Fujime and Maeda, 1985). Briefly speaking, Eq. 4 describes that D_{app} for Gaussian coils increases with x (see Eq. 7 given below) and hence K. The excess of D_{app} over D comes from contribution from the conformation fluctuations, the terms under the summation sign. Likewise, D_{app} for semiflexible rods increases with $k = KL/2$ (L, the rod length). The excess of D_{app} over D comes from contributions from the rotational and anisotropy in translational motions (R and A terms) and bending motions, the terms under the summation sign. These equations will be used in qualitative discussion of the experimental results.

The familiar Debye result of the scattering function, $P(x)$, for Gaussian coils is given by (Yamakawa, 1971)

$$P(x) = (2/x^2)[\exp(-x) - 1 + x], \quad (6)$$

$$x = K^2\langle R^2\rangle/6. \quad (7)$$

The Kirkwood formula for the translational diffusion coefficient, D, of Gaussian coils is given by (Yamakawa, 1971)

$$D = (k_BT/3\pi\eta L)[1 + 1.84(\gamma L)^{1/2}], \quad (8)$$

where k_B is the Boltzmann constant, T is the absolute temperature, η is the solvent viscosity, and the factor 1.84 comes from $(\zeta/6\pi\eta)(6/\pi)^{1/2}(8/3)$ for $(\zeta/6\pi\eta) = 1/2$ (the "segment number" in the original Kirkwood expression has been replaced with "γL" in Eq. 8 for our continuous chain model).

Throughout this paper, we expressed D and D_{app} (and any difference from and between them) in units of 10^{-8} cm^2/s. We also express K in units of 10^5 cm^{-1} and $\langle R^2\rangle$ in Eq. 1 in units of 10^{-10} cm^2. That is, $D = 3.60$, $K = 3$, and $\langle R^2\rangle = 3.0$, for example, mean 3.60×10^{-8} cm^2/s, 3×10^5 cm^{-1}, and 3.0×10^{-10} cm^2 respectively.

RESULTS

Effect on D_{app} of centrifugation of scattering samples

In our early stage of this study, a solution of connectin (0.5 – 1 mg/ml protein in 0.30 M NaCl and 0.25 M potassium phosphate buffer at pH 7.0) was first centrifuged at 39,000 *g* for 10 min and then carefully transferred to the scattering cell. Then, the DLS spectra were measured at several scattering angles from 30° to 120° (or several K values). A typical

example of D_{app} versus K relationships for such preparations is shown by filled circles in Fig. 2. (To emphasize the low K behavior of D_{app}, we display D_{app} against K, instead of conventional K^2, throughout this paper.) This relationship was compatible with that predicted by Eq. 4, but the estimated D value (i.e., D_{app} at $K = 0$) was unexpectedly small, about 2.3, in a sense that a combination of this D value with the sedimentation coefficient in literature gave a very large molecular mass of connectin molecule. This small D value might be due to the presence of aggregates of connectin molecules as well as dusts and microbubbles in scattering samples. Then, the solution was centrifuged at 39,000 g for 1 h (*open circles* in Fig. 2), 2 h (*triangles*), and 3 h (*squares*). The D_{app} values for these preparations became very much larger than those for the preparation centrifuged only for 10 min. The protein concentration was, for example, 0.86 and 0.77 mg/ml after centrifugation for 10 min and 1 h, respectively. The estimated D value for preparations after prolonged centrifugation was about 3.6, which gave a molecular mass of 3×10^6 Da for connectin molecule as discussed later. In what follows, therefore, we used the preparations centrifuged at 39,000 g for 2 h at least.

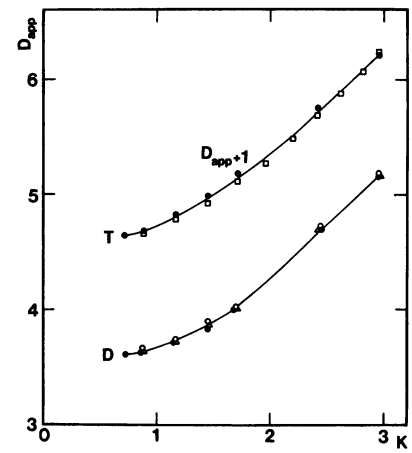

FIGURE 3 The D_{app} versus K relationships at 10°C. D denotes dilution experiments for preparation centrifuged at 39,000 × g for 2 h; connectin concentrations were 0.80 mg/ml (*filled circles*), 0.40 mg/ml (*triangles*), and 0.20 mg/ml (*open circles*). Label T denotes T/η scaling experiments (D_{app} values are displayed with shift by one unit); DLS measurements for 0.72 mg/ml solution after centrifugation at 39,000 × g for 3 h were made at 10°C (*squares*) and 31.6°C (*filled circles*; after T/η-corrected to 10°C). Solid lines are merely visual guides.

Effect on D_{app} of concentration of connectin

The D_{app} versus K relationships in Fig. 3 (label D) were obtained for the preparation centrifuged for 2 h; protein concentrations were 0.8 mg/ml (*filled circles*), 0.4 mg/ml (*triangles*), and 0.2 mg/ml (*open circles*). The dependence of D_{app} on protein concentrations was weak, but a slight tendency was observed that a lower concentration gave a little larger D_{app}.

(T/η) scaling of D_{app}

In order to see whether the so-called (T/η) scaling was valid or not for our samples, DLS measurements were made for preparation centrifuged for 3 h (0.72 mg/ml in this case). The D_{app} versus K relationships in Fig. 3 (label T) were obtained at sample temperatures of 10°C (*squares*) and 31.6°C (*filled circles*). The data at 31.6°C have been (T/η)-corrected to 10°C (the conversion factor from 31.6 to 10°C was as large as 1.83). A slight tendency was observed that higher temperature gave a little larger D_{app}. However, this was probably due to the fact that the sampling time t_s (31.6°C) was a little shorter than t_s (10°C)/1.83, and the scaling law seemed to hold for our preparation.

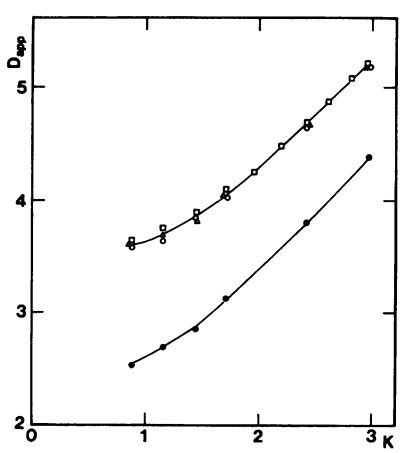

FIGURE 2 The D_{app} versus K relationships at 10°C. Connectin solutions were centrifuged at 39,000 × g for 10 min (*filled circles*; 0.86 mg/ml connectin), 1 h (*open circles*; 0.77 mg/ml connectin), 2 h (*triangles*), and 3 h (*squares*). Solid lines are merely visual guides.

Comparison of D_{app} versus K relationships of connectin and a semiflexible rod

The D_{app} versus K relationships depicted in Figs. 2 and 3 show quite a different feature from the D_{app} versus K relationship for a semiflexible rod with almost the same contour length L. One of us has reported the D_{app} versus K relationship for a dilute and monodisperse solution of fd virus (semiflexible rods) with the contour length of 895 nm and diameter (d) of 9 nm (Maeda and Fujime, 1985). The D_{app} versus K relationship for fd virus is shown in Fig. 4 (*filled circles*) after (T/η) correction to 10°C. The D_{app} versus K relationship for connectin is also shown in Fig. 4 (*open circles*), which was obtained for preparation centrifuged for 2 h (0.70 mg/ml protein). This measurement was made more extensively and carefully than those for Figs. 2 and 3; for given K (the scattering angle), many runs of 2-min duration were made to exclude accidental contributions of dusts and microbubbles at scattering angles of 25° and 30°, and to achieve high signal-to-noise ratios at high scattering angles. It should be noted that the D_{app} for connectin at the lowest K (at the scattering angle of 25°) was only very slightly smaller than that at the next lowest K (at 30°).

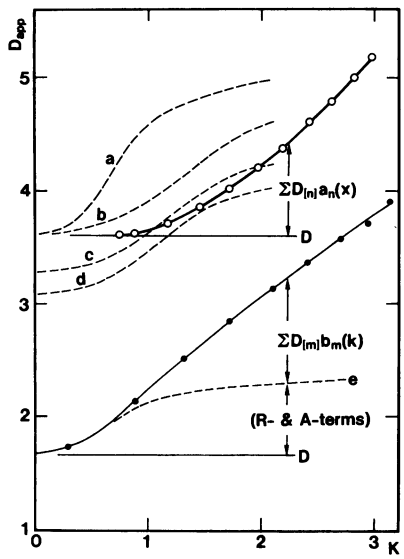

FIGURE 4 The D_{app} versus K relationships at 10°C. Open circles, 0.70 mg/ml connectin solution after centrifugation at 39,000 g for 2 h. The solid line connecting open circles is merely a visual guide. Filled circles, solution of 0.088 mg/ml fd virus (semiflexible rod with length L = 895 nm and diameter d = 9 nm); reproduced in a modified form with permission from Maeda and Fujime (1985) after being T/η-corrected to 10°C. The solid line connecting filled circles shows the simulated result for γL = 0.23 (Maeda and Fujime, 1985). Broken lines show the computed values of "D(Broersma) + (R and A terms)" in Eq. 5; (L and d in nanometer units) are (900, 0.05) for a, (450, 3.1) for b, (510, 3.1) for c, (550, 3.1) for d, and (895, 9) for e (fd virus).

First of all, we notice that the D value of connectin (3.60) is about 2.2 times larger than that of fd virus (1.66). For dimensions of fd virus, the Broersma formula for D of long rods (Broersma, 1969), $D = (k_BT/3\pi\eta L)[\ln(2L/d) - 0.73]$ (ignoring minor terms), gives 1.61 in a good agreement with the observed value of 1.66. On the other hand, if we assume connectin to be a semiflexible rod, the Broersma formula with D = 3.60 gives $2L/d \sim 5.7 \times 10^4$ or $d \sim 0.03$ nm (!!) for L = 900 nm. If we assume the d value of connectin to be 3 nm, which is in a range reported in literature (Maruyama et al., 1984; Nave et al., 1989), the Broersma formula does give D = 3.6 for L = 450 nm. But, these L and d values can not give the D_{app} versus K relationship for connectin (see the next paragraph for a quantitative discussion). On the other hand, if we use the Kirkwood formula for D of Gaussian coils, Eq. 8, we obtain γL = 25 or $\langle R^2\rangle$ = 3.18 = (178 nm)^2 for D = 3.60 and L = 900 nm. Noting $\langle R^2\rangle \sim L/\gamma$ and 1.84-$(\gamma L)^{1/2} \gg 1$ for large γL, the Kirkwood formula can be approximated as

$$D \approx 1.84(k_BT/3\pi\eta)\langle R^2\rangle^{-1/2}, \qquad (8')$$

which gives $\langle R^2\rangle$ = 2.63 = (162 nm)^2, or γL = 30 for L = 900 nm. These qualitative examinations strongly suggest that the connectin filament behaves hydrodynamically as a Gaussian coil.

Apart from differences in the absolute sizes of D_{app}, the dependence of D_{app} on K for connectin is quite different from that for fd virus. The broken lines in Fig. 4 show the computed values of D + (R and A terms) of Eq. 5 for various combinations of L and d (for algorithm, see Mochizuki-Oda and Fujime (1988)). Any of the broken lines with a (L = 900 nm, d = 0.05 nm), b (450 nm, 3.1 nm), c (510 nm, 3.1 nm), and d (550 nm, 3.1 nm) conflicts with the initial behavior of D_{app} against K for connectin. This again suggests that the connectin filament is a Gaussian coil. On the other hand, the broken line with e (L = 895 nm and d = 9 nm) does not conflict with the initial behavior of D_{app} against K for fd virus. The sum of the internal terms, $\Sigma D_{[n]}a_n(x) = D_{app} - D$, for connectin behaves against K in virtually the same fashion as that of the internal terms, $\Sigma D_{[m]}b_m(k) = D_{app} - D$ - (R and A terms), for fd virus does. Therefore, the difference in the initial behaviors of the D_{app} versus K relationships for connectin and fd virus is solely due to the absence of (R and A terms) in the former. The K dependence of D_{app} for connectin can hardly be explained by a theoretical model for semiflexible rods.

Estimation of $\langle R^2\rangle$ for connectin in solution

The K dependence of the static scattering intensity $I(K)$ would provide us information about the mean-square radius of gyration, $\langle R_g^2\rangle$ (= $\langle R^2\rangle/6$ for Gaussian coils and $L^2/12$ for rods). The low K behavior of $I(K)$ is given by $I(K) = 1 - \frac{1}{3}\langle R_g^2\rangle K^2 + \ldots$ irrespective of the conformation of the scatterers (Yamakawa, 1971). The I versus K relationship for connectin is shown in Fig. 5. Because of technical difficulties, our measurements were not carried out down to sufficiently small K values. So, the observed I versus K relationship was simply compared with $k_sP(x)$, where k_s is the scale factor and $P(x)$ is given by Eq. 6. The computed $k_sP(x)$s are shown in Fig. 5 for $\langle R^2\rangle$ = 2.80 (label a), 2.70 (label b), and 2.60 (label c). This result suggests $\langle R^2\rangle$ = 2.60–2.70 = (160 nm)^2. Equation 1, or $\langle R^2\rangle = 2L^2(2\gamma L - 1)/(2\gamma L)^2$ for

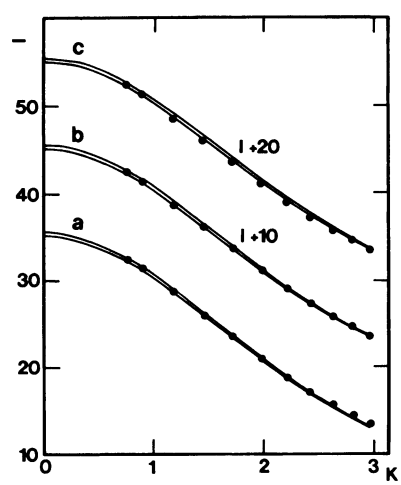

FIGURE 5 The I versus K relationships. The static scattering intensities (*filled circles*, in arbitrary units) were taken from data in Fig. 3. Solid lines show $k_sP(x)$ for $\langle R^2\rangle$ (= 2.80 for label a, 2.70 for label b, and 2.60 for label c) and k_s (= 35.5 and 30 for each set of lines). Both observed points and solid lines are displayed with shift by 10 units for label b and 20 units for label c.

$\gamma L > 5$, gives $\gamma L = 30$ for $\langle R^2 \rangle = 2.66 = (163\ \text{nm})^2$ and the assumed value of $L = 900$ nm.

A theoretical formulation for the field correlation function, $g^1(t)$, of light scattered from monodisperse solution of Gaussian coils was first described by Pecora (1968), who adopted a bead-and-spring model without the hydrodynamic interaction between beads. We developed the same formulation in terms of a worm-like chain model without the hydrodynamic interaction (Maeda and Fujime, 1980), and with the preaveraged one (Fujime and Higuchi, 1993). Following the method detailed in the latter (Fujime and Higuchi, 1993), we computed $g^1(t)$s for given parameter values of $D = 3.60$ and $\langle R^2 \rangle$ from 2.50 to 2.80. Then, the constructed $G^2(mt_s) = 1 + [g^1(mt_s)]^2$ were analyzed by the the same program as that used in the experiment. The D_{app} versus K relationships thus simulated are compared with the experimental points in Fig. 6. The analysis of the contribution to D_{app} from internal modes of motion suggests again $\langle R^2 \rangle = 2.60$–$2.70$.

DISCUSSION

Remarks on some technical problems

In the field of polymer physics and chemistry, the size of the radius of gyration is routinely estimated from the low K behavior of $I(K)$ because of its model independence. Unfortunately, we could not do so. However, the estimated size of $\langle R^2 \rangle = 2.60$–$2.70$ from overall fitting with $I(K) = k_s P(x)$ agreed with that from the analysis of the D_{app} versus K relationships. This agreement is remarkable, because only the high K behavior of D_{app} can provide information about internal modes of motion. From the observed value of $D = 3.60$ at 10°C, we have the Stokes radius of $R_s = (k_B T/6\pi\eta D) = 44.1$ nm. On the other hand, the radius of gyration is estimated to be $R_g = (\langle R^2 \rangle/6)^{1/2} = 66.6$ nm for $\langle R^2 \rangle = 2.66$. Then, we have the ratio $R_g/R_s = 1.51$, of which size is characteristic of Gaussian coils, i.e., $R_g/R_s = (8/3\pi^{1/2}) = 1.50$ for Gaussian coils (Yamakawa, 1971). Since the estimation of R_s from the observed D value is independent of model (coil or rod), the ratio of 1.51 assures the present analyses based on formulas for Gaussian coils. In the analyses given above for static and dynamic light-scattering data, we implicitly assumed a monodisperse size distribution of connectin molecules. Possible effects of sample polydispersity have also been discussed elsewhere (Fujime and Higuchi, 1993): Referring to the description in Nave et al. (1989) for their electron microscopic observation of β-connectin, we assumed a unimodal length distribution for which $L/L_n = 1.00 \pm 0.30$ and $L_w/L_n = 1.09$ (L_n and L_w being the number- and weight-averaged lengths, respectively). Although this assumed distribution may be the worst one for our preparation, however, the analyses of D_{app} versus K and I versus K relationships again gave $\langle R^2 \rangle = 2.66$ as quoted in Table 1.

Estimation of molecular mass

The molecular mass M is related to the sedimentation coefficient s and the translational diffusion coefficient D by

$$M = [k_B T N_A/(1 - v\rho)](s/D), \qquad (9)$$

where N_A is the Avogadro number, v is the specific volume, and ρ is the density of solvent. The present result for D of connectin is 3.60 (and 3.65 at the infinite dilution) at 10°C, which equals 4.87 (4.94) at 20°C in water. If we assume $v\rho = 0.73$ (a typical value for proteins in water), Eq. 9 gives $M = 3{,}150$–$3{,}100$ kDa for the literature value of $s_{20,w} = 17$ S in 0.1 M phosphate buffer, pH 7.0 (Maruyama et al., 1984). The light-scattering D value is the z average over size distribution, whereas the s value is the weight average. If this fact is taken into account, the number-averaged molecular mass of connectin is close to but a little smaller than 3.0 MDa. Since we did not measure the s value (and also the v value) for our own sample in the *same* solvent as that in DLS measurements, we do not argue the size of the above M value. We just claim that the present M value strongly supports our implicit assumption of molecular dispersion of connectin filaments in solution after prolonged centrifugation (Fig. 1).

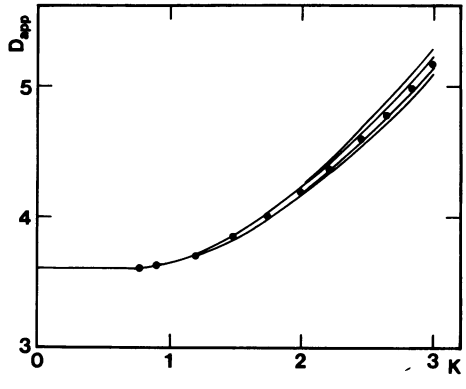

FIGURE 6 Simulated D_{app} versus K relationships at 10°C. Solid lines from top to bottom are for $\langle R^2 \rangle = 2.80$, 2.70, 2.60, and 2.50 (and $\gamma L = 30$). Filled circles were taken from Fig. 3.

Table 1 Summary of the analysis of light-scattering results.

Methods	Given L	Estimated γL	Estimated $\langle R^2 \rangle$
	nm		
K (Kirkwood) = D (observed)*			
(Eq. 8)	$L = 900$	$\gamma L = 25$	$3.18 = (178\ \text{nm})^2$
(Eq. 8′)			$2.63 = (162\ \text{nm})^2$
$I(K) = k_s P(x)$			
(Monodisperse)*			$2.7 = (160\ \text{nm})^2$
(Polydisperse)‡			$2.6 = (160\ \text{nm})^2$
D_{app} versus K			
(Monodisperse)*‡			$2.65 = (163\ \text{nm})^2$
(Monodisperse)‡	$L = 900$	$\gamma L = 30$	$2.66 = (163\ \text{nm})^2$
	$= 800$	$= 23.5$	$2.67 = (163\ \text{nm})^2$
(Polydisperse)‡	$L_W = 900$	$\gamma L_W = 30$	$2.66 = (163\ \text{nm})^2$

* This study.

‡ From Fujime and Higuchi (1993). Mono- and polydisperse mean that analyses were made by assuming mono- and polydisperse length distributions of connectin filaments, respectively.

The present M value is close to but slightly larger than those from sedimentation equilibrium experiments, 2.7 MDa for native β-connectin (Maruyama et al., 1984) and 2.6 MDa for a mixture of roughly equal amounts of titin-1 and -2 in 6 M guanidine-HCl (Kurzban and Wang, 1988), but distinctly different from an SDS-PAGE result for 2% polyacrylamide gels, 2.1 MDa (Maruyama et al., 1984). The slight differences among the former three values may be due to different methods for different preparations in different solvents. The very small value of 2.1 MDa may be largely due to a difference in electrophoretic behaviors of a superlong polypeptide and star-branched markers of cross-linked myosin heavy chains used in Maruyama et al. (1984). In fact, 2.6 and 2.8 MDa (for β-connectin) were obtained, respectively, for 1.6 and 1.5% polyacrylamide gels in the presence of 0.3% agarose (Hu et al., 1989); suggesting M reaching to 3 MDa in sufficiently soft gels.

Flexural rigidity and persistence length

As summarized in Table 1, the present result gives $\langle R^2 \rangle^{1/2} =$ (163 nm), which is much smaller than $L = 900$ nm, for example. Equation 1 gives $\gamma L = 30$. Then, the statistical segment length (γ^{-1}) will be 30 nm. Namely, one segment length covers eight contiguously repeating domains with 4-nm size each (Funatsu et al., 1993). (The statistical segment length may or may not have some structural relation with the 44-nm superrepeats (Labeit et al., 1992) mentioned in Introduction.) Here, the following should be stressed: the size of $\gamma^{-1} = 30$ nm was obtained with the implicit assumption of $L = 900$ nm. Since we did not examine the size distribution of our own sample, it is not clear whether this assumption was valid or not. However, because the size of $\langle R^2 \rangle$ can be estimated without the exact L value (see Figs. 5 and 6; see also Fujime and Higuchi (1993)) and an approximate relation $\langle R^2 \rangle \sim L/\gamma$ holds, the estimation of γ^{-1} (and hence L_p, ϵ, and k discussed below) can be determined within a factor of 1.5 at the worst; i.e., $\gamma^{-1} \sim 45$ nm even if $L =$ 600 nm. Therefore, the discussion given below is essentially valid regardless of the true contour length of connectin filaments in our preparations.

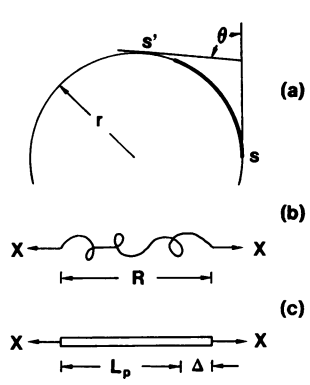

FIGURE 7 (*a*) A diagram defining the angle θ between the directions of two tangents at s and s' along a worm-like chain, where the thick portion with length L_p is assumed, for a qualitative consideration, to lie on the circle with radius r. (*b*) A diagram illustrating a worm-like chain of which end-to-end distance R ($[<] L$) is stretched by an external force X. (*c*) A diagram illustrating a worm-like chain of which contour length is stretched by an external force X, where L_p is the persistence length and Δ is its extension.

The elastic potential energy V of a worm-like chain is defined by

$$V(\sigma) = \frac{\epsilon}{2} \int r(s)^{-2}\, ds \tag{10}$$

where ϵ (dyn × cm^2) is the flexural rigidity, $r(s)$ is the radius of curvature at s along the chain (Fig. 7 *a*), $\sigma = |s - s'|$ and the integration range is $[0, \sigma]$. Let $\mathbf{e}(s)$ be the unit vector parallel with the tangent to the chain at s and θ be the angle between two tangents (Fig. 7 *a*). For the potential energy defined by Eq. 10, the average of $\cos(\theta)$ over all possible conformations is given by (Yamakawa, 1971)

$$\langle \cos(\theta) \rangle \equiv \langle \mathbf{e}(s) \cdot \mathbf{e}(s') \rangle = \exp(-2\gamma\sigma), \tag{11}$$

where $\gamma = k_B T/(2\epsilon)$. (The integration of Eq. 11 over s and s' in the range $[0, L]$ gives Eq. 1.) The correlation between the directions of tangents decays with separation σ, and $\langle \cos(\theta) \rangle$ is equal to e^{-1} for $\sigma = L_p$ (this is a definition of the "persistence" length L_p); $L_p = (2\gamma)^{-1}$. Namely, the persistence length is just the half of the Kuhn statistical segment length. By use of this definition of L_p, the flexural rigidity is given by

$$\epsilon = k_B T L_p. \tag{12}$$

This relation can be derived approximately in a qualitative manner as follows. From $\langle \cos(\theta_c) \rangle = e^{-1}$ we have $\theta_c = 68.4°$. For simplicity, we assume that the worm-like chain with length L_p lies along the circle with radius r (Fig. 7 *a*). We then have a relation $2\pi r \times (68.4°/360°) = L_p$, or $r = 0.84\, L_p$, and the thermal average of the potential energy is given by $\langle V(L_p) \rangle = (\epsilon/2) r^{-2} L_p$ (cf. Eq. 10). From the equipartition theorem in statistical physics (Kittel, 1958), we have $\langle V \rangle = k_B T$, and hence $\epsilon = 2(0.84)^2 k_B T L_p \sim k_B T L_p$.

For $\gamma^{-1} = 30$ nm ($L_p = 15$ nm) Eq. 12 gives $\epsilon = 6.0 \times 10^{-20}$ dyn × cm^2. This size of $\epsilon = 6$ (in units of 10^{-20} dyn × cm^2) for connectin should be compared with those of $\epsilon =$ 1900 for muscle thin filaments (re-evaluated for $D = 1.64$ instead of 1.0 in Fujime et al. (1979)), 780 for fd virus (Maeda and Fujime, 1985), 68 for collagen (Kubota et al., 1987), 63 for poly(γ-benzyl L-glutamate) in dimethylformamide (PBLG in DMF, an α-helical polymer) (Kubota et al., 1986), 22 for DNA (Elias and Eden, 1981), and theoretical estimates for α-helical polypeptides; 41 for poly(L-alanine) and 25 for polyglycine (Suezaki and Go, 1976). Namely, the flexural rigidity of connectin is an order of magnitude smaller than those of collagen, α-helical polypeptides and DNA. The high flexibility (small size of ϵ) of connectin is compatible with the fact that the molecule does not contain any α-helical structure but consists mostly of β-sheet structure (Maruyama, 1986).

Extension of end-to-end distance under external force

When an external force X is applied, both ends of a Gaussian coil is stretched to a distance R (Fig. 7 *b*). In such a situation, we have a relation $R/(Nb) = L(bX/k_BT)$ (Yamakawa, 1971), which is rewritten in our continuous chain model as $R/L = L(X/k_BT\gamma)$, where $L = Nb$ and $b = \gamma^{-1}$ as mentioned in Introduction, and $L(u) = \coth(u) - 1/u$ is the Langevin function. This relation can be extremely simplified in two cases (i.e., $L(u) = u/3$ for small u, and $L(u) = 1 - 1/u$ for $u > 5$);

$$R/L = X/(3k_BT\gamma) \qquad \text{for small } X, \tag{13a}$$

$$= 1 - k_BT\gamma/X \qquad \text{for } X > 5k_BT\gamma. \tag{13b}$$

Since $k_BT\gamma = 0.13$ pN for $\gamma^{-1} = 30$ nm, Eq. 13a predicts that a force $X \sim 0.13$ pN stretches a connectin filament to $R/L \sim 1/3$. On the other hand, Eq. 13b gives $R/L = 0.90$ and 0.96 for $X = 1.3$ and 3.5 pN, respectively. In other words, a force of a few pico-Newtons stretches a single connectin filament to an almost straightened state.

Extension of contour length under external force

When the external force is larger than a few pico-Newtons, we have to consider an extension of the contour length. Based on elementary considerations (Fujime et al., 1979), the elastic constant is roughly estimated for the connectin filament stretched to a length longer than L. For a macroscopic uniform rod with diameter d, the flexural rigidity ϵ is equal to the product of the Young modulus Y and the moment of inertia I ($= \pi d^4/64$) of the cross-section of the rod, i.e., $\epsilon = YI$. If this relation is applied to a fibrous protein, the Young modulus Y obtained from ϵ is related to the microscopic elastic constant k. If, under an external force X, the worm-like chain with length L_p is stretched by Δ (Fig. 7 *c*), we have the Hookean relation $X = k\Delta$. Therefore, the relation between Y and k is given by $Y = kL_p/A$, where A is the cross-sectional area of the rod and use was made of the definition of $Y \equiv (X/A)/(\Delta/L_p)$. Since $A = \pi(d/2)^2$, we finally have

$$k = 16\epsilon/(d^2L_p) = 16k_BT/d^2 = 7 \text{ dyn/cm} \tag{14}$$

for one persistence length of a single connectin filament with $d = 3$ nm. An external force of $X = 60$ pN $= 60 \times 10^{-7}$ dyn induces the extension of L_p by $\Delta = 8.6$ nm, or of contour length ($L = 60\ L_p$) by $60\Delta = 510$ nm (by assuming no limitation of Hookean relation $X = k\Delta$, but see the next subsection). This high extensibility of the contour length may arise from that of each 4-nm domain and/or that of the interface between domains. Which is dominant, intra- or interdomain extensibility? The present result does not give any conclusive answer about this, because we obtained only the size of L_p.

For collagen with $L_p = 170$ nm and hydrodynamic diameter of $d = 2.2$ nm (Kubota et al., 1987), Eq. 14 gives $k = 13$ dyn/cm (per L_p) and $k' \equiv (L_p/15)k = 150$ dyn/cm (per 15 nm). For PBLG in DMF with $L_p = 157$ nm and hydrodynamic diameter of $d = 2.2$ nm (Kubota et al., 1986), we have $k = 13$ dyn/cm (per L_p) and $k' = 140$ dyn/cm (per 15 nm). Namely, the elastic constant $k\ (= k')$ = 7 dyn/cm (per $L_p = 15$ nm) for connectin is an order of magnitude smaller than k' for collagen and PBLG in DMF.

The β-spiral structure in an elastin fiber, a famous biological elastic fiber, was once considered to be one of candidates for an elastic structure present in connectin, since connectin is rich in β-sheet structure (Maruyama, 1986). Therefore, it is also interesting to compare the elastic moduli of connectin with those of elastin. The Young modulus Y of purified fibrous elastin from bovine ligamentum nuchae has been reported to be 1×10^6 to 3×10^6 dyn/cm^2 depending on the degree of extension (Urry, 1984). To estimate ϵ and k' from Y, sizes of A and d of elastin are needed. For this purpose, crystallographic data of cyclopentadecapeptide can be used; the hexagonal unit cell of $a = 2.85$ nm, $c = 1.00$ nm, and $Z = 3$ (Cook et al., 1980). The area of the basal plane of the unit cell is calculated to be $A_{unit} = (3^{1/2}/2)a^2 = 7.0 \times 10^{-14}$ cm^2, so that we have $A = A_{unit}/Z = 2.3 \times 10^{-14}$ cm^2 and $d = 1.7$ nm from $\pi(d/2)^2 = A$. We then have $\epsilon = 0.4 \times 10^{-22}$ to 1.3×10^{-22} dyn $\times$ cm^2 and $k' = 0.02$–0.05 dyn/cm (per 15 nm). Since the sizes of A and d used here are their upper bounds, because of neglect of intermolecular space (although not very much) in the unit cell, the above estimates of ϵ and k' for elastin should also be their upper bounds. Nevertheless, these elastic moduli of elastin are two orders of magnitude smaller than those of connectin. An almost complete (T/η) scaling was observed for connectin in the temperature range 10° to 32°C (label T in Fig. 3); no changes in molecular parameter (γ or $\langle R^2 \rangle$) and dispersion (aggregation/disaggregation) in the temperature range studied. This is in contrast with the fact that a rise in temperature to a few degrees above 20°C results in an increase in intermolecular order of elastin (Urry, 1984). Furthermore, it was recently suggested that some of β-sheets in a connectin fiber were aligned with their mainchain axes parallel to the fiber axis (Uchida et al., 1991), and the same also in fibronectin type III domain (Leahy et al., 1992). From these mechanical, thermodynamical, and structural points of view, it turns out that the β-spiral structure proposed for elastin is improbable in connectin.

Resting tension of mechanically skinned muscle fiber at extreme stretch

β-Connectin is an in situ proteolytic product of the mother molecule (α-connectin or titin 1); the former is a little longer than three quarters of the latter (Maruyama, 1986). About two thirds (in length) of each β-connectin filament are bound to a thick filament. Namely, the missing part (by proteolysis) and only one third (in length) of β-connectin can contribute to the elastic component in muscle. It is therefore important to know whether the elastic property is homogeneous along α-connectin or not. When skinned fibers are treated with a high ionic-strength solution, each thick filament partially dis-

solves from both ends (Ishiwata, 1981). This may result in an increase in the length of β-connectin which can contribute to the resting tension T_C. A comparison of the T_C versus sarcomere length (SL) relationships of skinned fibers with and without this treatment has suggested that the elastic property of the missing part in question is almost the same as that of β-connectin (Higuchi et al., 1992). An electron microscopic observation at high resolution has also suggested that elongation of the 4-nm domains in a stretched fiber is almost the same for those near Z-lines and those near A-bands (Funatsu et al., 1993). In what follows, therefore, the elastic property of any portion along α-connectin is assumed to be the same as that along β-connectin.

At $SL = 2.2$ μm, the 1, 0 lattice spacing, $d_{1,0}$, of a mechanically skinned fiber of frog muscle is about 42 nm (Higuchi and Umazume, 1986), which gives the unit cell area of $A_{unit} = 2d_{1,0}^2/3^{1/2} = 2.0 \times 10^{-15}$ m^2. Since myofilaments occupy only ~80% of the cross-sectional area of a myofibril (Schoenberg, 1980), the number of thick filaments is estimated to be $N_T = 0.8/A_{unit} = 4.0 \times 10^{14}$ (filaments/m^2). Taking molecular mass of connectin and myosin as 3×10^6 and 5×10^5 Da, their contents of 10 and 44% in the total myofibrillar proteins, and 300 myosin monomers to form a thick filament, the presence of 12 connectin filaments per thick filament is calculated; it is expected that six connectin filaments are present in each half of the thick filament (Maruyama, 1986). The cross-sectional density of connectin will be $N_C = 6N_T = 2.4 \times 10^{15}$ m^{-2}.

The contribution of connectin filaments to the resting tension of a mechanically skinned fiber of frog muscle has been estimated to be T_C ~0.3×10^4, 0.6×10^4, and 1.7×10^4 N/m^2 at $SL = 2.8$, 3.0, and 3.5 μm, respectively (Higuchi and Umazume, 1985). If a single connectin filament is assumed to contribute to the resting tension independently of each other, the filament is expected to develop tension $X = T_C/N_C \sim 1.3$, 2.6, and 7 pN at $SL = 2.8$, 3.0, and 3.5 μm, respectively. Then, the small value of the resting tension at $SL < 2.8$ μm can be described by the extension of R ($< L$). As mentioned before, on the other hand, the sizes $X \sim 2.6$ and 7 pN of the external force are large enough for a single connectin filament to be almost straightened ($R/L \sim 1$). In a model of connectin filaments in a sarcomere (for example, Fig. 11 in Maruyama (1986)), the filaments are almost straightened at $SL = 2.6$ μm. In discussing mechanical properties of in situ connectin filaments, therefore, the behavior of the resting tension of mechanically skinned fibers against changes in SL has to be taken into account (Higuchi and Umazume, 1985). When a skinned fiber at $SL = 3.5$ μm is quickly stretched to $SL = 4.5$ μm, for example, the resting tension instantly increases to a very large value (depending on the rate of stretching), and then decreases, first quickly and then slowly, to a small value of T_C ~2.5×10^4 N/m^2; a stress relaxation. When the fiber at $SL = 4.5$ μm after stress relaxation is shortened to $SL = 4$ μm, for example, it shows a much smaller T_C than that shown by a virgin fiber; a large hysteresis in the T_C versus SL relationship. In any model proposed for connectin filaments in a sarcomere (e.g., Higuchi and Umazume, 1985 and 1986; Maruyama, 1986; Trinick, 1991; Wang et al., 1991; Higuchi et al., 1992; Funatsu et al., 1993), the filaments must be stretched by more than 500 nm when SL is changed from 3.5 to 4.5 μm. Such an extreme extension of individual filaments would produce an additional force $X > 120$ pN per filament as estimated before, or $T_C > 2.8 \times 10^5$ N/m^2 (here about 500-nm portion of each connectin filament free from binding to a thick filament was assumed to be stretched).

To account for an order of magnitude difference between the sizes of T_C, i.e., $>2.8 \times 10^5$ N/m^2 expected from $N_C X = N_C k\Delta$ and $\sim 2.5 \times 10^4$ N/m^2 observed after stress relaxation, the following situations (and also *equivalent* ones) can be plausible: one is that when the fiber is extremely stretched, each connectin produces a large force, say >120 pN, so that its connections to a Z-line and/or to a thick filament are broken down, and/or it is lengthened irreversibly; resulting in a decrease of the number of active filaments in a sarcomere. The other and more likely model is a two-state (or more generally a multi-state) one. Under a high tension, the conformation of connectin changes from one state C_R to the other C_T. The C_R state that is stable under no (and small) external force gives the domain size L_R (= 4 nm) and the elastic constant k_R (= $(L_p/L_R)k$, with $k = 7$ dyn/cm). On the other hand, the C_T state is assumed to give a domain size L_T and an elastic constant k_T, which are (several times) longer and larger than L_R and k_R, respectively. When the filament is stretched, each C_R domain is stretched to $L_R + \delta$. If the force X ($= k_R\delta$) induces the transformation of some C_R domains in each single filament to C_T domains, the size of δ becomes small because of $L_T > L_R$, resulting in a decrease of X. If δ- (or X-)dependent rate constants for transition between C_R and C_T states are suitably defined, the fast and slow processes of stress relaxation may be described. When the stretched filament is relaxed, some C_T domains will transform to C_R domains. If the rate constants are also defined in such a way that a certain stage of this process is very slow, an apparent hysteresis may be described.

Although the above two- (multi-)state model may account for superhigh extensibility of the connectin filament under an external force, it is nothing but speculative at present. It should be noted, however, that the domain size increases by ~20% when the distance between the Z-line and A-band increases by ~100% (Funatsu et al., 1993). This may be partly due to the fact that elastic filaments are slack in short SL (Funatsu et al., 1993) and/or due to the fact that the number of C_T domains increases with SL. The average force-bearing capacity for the extensible segment was recently reported to be 25 pN per single connectin filament at the "yield point" (Wang et al., 1993). The size of this yield point force is about one fourth of $X = k\Delta$, suggesting again transition of some domains from C_R to C_T states. In any case, it seems to be important to examine in detail the stress relaxation and hysteresis in the T_C versus SL relationship of mechanically

skinned fibers on the one hand, and the domain size distribution of highly stretched connectin filaments along their entire length on the other hand.

Concluding remarks

We have characterized the isolated connectin filaments in solution by means of DLS spectroscopy. Both static and dynamic light-scattering data gave $\langle R^2 \rangle = (163 \text{ nm})^2$. Then, Eq. 1 gives $L_p = 15$ nm for assumed value of $L = 900$ nm. Once L_p is known, we can estimate the flexural rigidity $\epsilon = 6.0 \times 10^{-20}$ dyn $\times$ cm^2 and the elastic constant for extension $k = 7$ dyn/cm (per L_p). Both ϵ and k of connectin (under no and small external force) are an order of magnitude smaller than those of collagen and α-helical polypeptides, but two orders of magnitude larger than those of elastin. Taking the size of k for connectin into account, we have qualitatively examined the resting tension T_C developed by mechanically skinned muscle fibers stretched to large sarcomere lengths SL; a force-dependent conformational change in connectin appears to be a candidate to account for superhigh extensibility of connectin, low T_C after stress relaxation and hysteresis in the T_C versus SL relationship.

REFERENCES

Berne, B., and R. Pecora. 1975. Dynamic Light Scattering. Interscience, New York. 376 pp.

Broersma, S. J. 1969. Viscous force constant for a closed cylinder. *J. Chem. Phys.* 32:1632–1635.

Chu, B. 1974. Laser Light Scattering. Academic Press Inc., New York. 317 pp.

Cook, W. J., H. Einspahr, T. L. Trapane, D. W. Urry, and C. E. Bugg. 1980. Crystal structure and conformation of cyclic trimer of a repeat pentapeptide of elastin, *cyclo*-(L-valyl-L-prolylglycyl-L-valylglycyl)$_3$. *J. Am. Chem. Soc.* 102:5502–5505.

Elias, J. G., and D. Eden. 1981. Transient electric birefringence study of the persistence length and electrical polarizability of restriction fragments of DNA. *Macromolecules.* 14:410–419.

Fairbanks, G., T. L. Steck, and D. F. H. Wallach. 1971. Electrophoretic analysis of the major polypeptide of the human erythrocyte membrane. *Biochemistry.* 10:1607–1617.

Fujime, S., and H. Higuchi. 1993. An analysis of dynamic light-scattering spectra of wormlike chains: β-connectin from striated muscle. *Macromolecules.* In press.

Fujime, S., S. Ishiwata, and T. Maeda. 1984. Dynamic light scattering study of muscle F-actin. *Biophys. Chem.* 20:1–20.

Fujime, S., and T. Maeda. 1985. Spectrum of light quasi-elastically scattered from dilute solutions of very long and slightly bendable rods. Effect of hydrodynamic interaction. *Macromolecules.* 18:191–195.

Fujime, S., S. Yoshino, and Y. Umazume. 1979. Optical diffraction study on the dynamics of thin filaments in skinned muscle fibers. *In* Cross-Bridge Mechanism in Muscle Contraction. H. Sugi and G. H. Pollack, editors. University of Tokyo Press, Tokyo. 51–67.

Funatsu, T., H. Higuchi, and S. Ishiwata. 1990. Elastic filaments in skeletal muscle revealed by selective removal of thin filaments with plasma gelsolin. *J. Cell Biol.* 110:53–62.

Funatsu, T., E. Kono, H. Higuchi, S. Kimura, S. Ishiwata, T. Yoshioka, K. Maruyama, and S. Tsukita. 1993. Elastic filaments in situ in cardiac muscle; deep-etch replica analysis in combination with selective removal of actin and myosin filaments. *J. Cell Biol.* 120:711–724.

Higuchi, H., and Y. Umazume. 1985. Localization of the parallel elastic components in frog skinned muscle fibers studied by the dissociation of the A- and I-bands. *Biophys. J.* 48:137–147.

Higuchi, H., and Y. Umazume. 1986. Lattice shrinkage with increasing resting tension in stretched single skinned fibers of frog muscle. *Biophys. J.* 50:385–389.

Higuchi, H., T. Suzuki, S. Kimura, T. Yoshioka, K. Maruyama, and Y. Umazume. 1992. Localization and elasticity of connectin (titin) filaments in skinned frog muscle fibres subjected to partial depolymerization of thick filaments. *J. Muscle Res. Cell Motil.* 13:285–294.

Horowits, R., and R. J. Podolsky. 1987. The positional stability of thick filaments in activated skeletal muscle depends on sarcomere length: evidence for the role of titin filaments. *J. Cell Biol.* 105:2217–2223.

Horowits. R., K. Maruyama, and R. J. Podolsky. 1989. Elastic behavior of connectin filaments during thick filament movement in activated skeletal muscle. *J. Cell Biol.* 109:2169–2176.

Hu, D. H., S. Kimura, and K. Maruyama. 1989. Myosin oligomers as the molecular mass standard in the estimation of molecular mass of nebulin (~800 kDa) by sodium dodecylsulfate-polyacrylamide gel electrophoresis. *Biomed. Res.* 10:165–168.

Ishiwata, S. 1981. Melting from both ends of an A-band in a myofibril. Observation with a phase-contrast microscope. *J. Biochem. (Tokyo).* 89: 1647–1650.

Itoh, Y., S. Kimura, T. Suzuki, K. Ohashi, and K. Maruyama. 1986. Native connectin from porcine cardiac muscle. *J. Biochem. (Tokyo).* 100: 439–447.

Kittel, C. 1958. Elementary Statistical Physics. John Wiley & Sons, Inc., New York. 228 pp.

Kubota, K., Y. Tominaga, and S. Fujime. 1986. Quasielastic light-scattering study of semiflexible polymers. Poly(γ-benzyl L-glutamate) in dimethylformamide. *Macromolecules.* 19:1604–1612.

Kubota, K., Y. Tominaga, and S. Fujime. 1987. Dynamic light-scattering study of semiflexible polymers: collagen. *Biopolymers.* 26: 1717–1729.

Kurzban, G. P., and K. Wang. 1988. Giant polypeptides of skeletal muscle titin. Sedimentation equilibrium in guanidine hydrochloride. *Biochem. Biophys. Res. Commun.* 150:1155–1161.

Labeit, S., D. P. Barlow, M. Gautel et al. 1990. A regular pattern of two types of 100-residue motif in the sequence of titin. *Nature (Lond).* 345:273–276.

Labeit, S., M. Gautel, A. Lakey, and J. Trinick. 1992. Towards a molecular understanding of titin. *EMBO J.* 11:1711–1716.

Leahy, D. J., W. A. Hendrickson, I. Aukhil, and H. P. Erickson. 1992. Structure of a fibronectin type III domain from tenascin phased by MAD analysis of the selenomethionyl protein. *Science (Washington DC).* 258: 987–991.

Maeda, T., and S. Fujime. 1980. Effect of filament flexibility on the dynamic light-scattering spectrum with special reference to fd virus and muscle thin filaments. *Macromolecules.* 14:809–818.

Maeda, T., and S. Fujime. 1985. Dynamic light-scattering study of suspensions of fd virus. Application of a theory of the light-scattering spectrum of weakly bending filaments. *Macromolecules.* 18:2430–2437.

Maruyama, K. 1986. Connectin, an elastic filamentous protein of striated muscle. *Int. Rev. Cytol.* 104:81–114.

Maruyama, K., S. Kimura, H. Yoshidomi, H. Sawada, and M. Kikuchi. 1984. Molecular size and shape of β-connectin, an elastic protein of striated muscle. *J. Biochem. (Tokyo).* 95:1423–1433.

Maruyama, K., S. Matsubara, R. Natori, Y. Nonomura, S. Kimura, K. Ohashi, F. Murakami, S. Handa, and G. Eguchi. 1977. Connectin, an elastic protein of muscle: characterization and function. *J. Biochem. (Tokyo).* 82:317–337.

Mochizuki-Oda, N., and S. Fujime. 1988. Dynamic light-scattering study of synthetic myosin filaments. *Biopolymers.* 27:1389–1401.

Nave, R., D. O. Furst, and K. Weber. 1989. Visualization of the polarity of isolated titin molecules: a single globular head on a long thin rod as the M band anchoring domain? *J. Cell Biol.* 109:2177–2187.

Pecora, R. 1968. Spectral distribution of light scattered from flexible-coil macromolecules. *J. Chem. Phys.* 49:1562–1564.

Schmitz, K. S. 1990. An Introduction to Dynamic Light Scattering by Macromolecules. Academic Press Inc., New York. 449 pp.

Schoenberg, M. 1980. Geometrical factors influencing muscle force development. II. Radial forces. *Biophys. J.* 30:69–78.

Suezaki, Y., and N. Go. 1976. Fluctuations and mechanical strength of α-helices of polyglycine and poly(L-alanine). *Biopolymers.* 15:2135–2153.

Trinick, J. 1991. Elastic filaments and giant proteins in muscle. *Curr. Opin. Cell Biol.* 3:112–119.

Uchida, K., I. Harada, Y. Nakauchi, and K. Maruyama. 1991. Structural properties of connectin studied by ultraviolet resonance Raman spectroscopy and infrared dichroism. *FEBS Lett.* 295:35–38.

Urry, D. W. 1984. Protein elasticity based on conformations of sequential polypeptides: the biological elastic fiber. *J. Protein Chem.* 3:403–436.

Wang, K. 1985. Sarcomere-associated cytoskeletal lattices in striated muscle. Reviews and hypothesis. *In* Cell and Muscle Motility, Vol. 6. Shay, J. W., editor. Plenum Publishing, New York. 315–369.

Wang, K., R. McCarter, J. Wright, J. Beverly, and R. Ramirez-Mitchell. 1991. Regulation of skeletal muscle stiffness and elasticity by titin isoforms: a test of the segmental extension model of resting tension. *Proc. Natl. Acad. Sci. USA.* 88:7101–7105.

Wang, K., R. McCarter, J. Wright, J. Beverly, and R. Ramirez-Mitchell. 1993. Viscoelasticity of the sarcomere matrix of skeletal muscles. The titin-myosin composite filament is a dual-stage molecular spring. *Biophys. J.* 64:1161–1177.

Yamakawa, H. 1971. Modern Theory of Polymer Solutions. Harper and Row, New York. 419 pp.